MNRAS **456,** 2636–2646 (2016) doi:10.1093/mnras/stv2821

The detailed chemical composition of the terrestrial planet host Kepler-10★

F. Liu,[1]† D. Yong,[1] M. Asplund,[1] I. Ramírez,[2] J. Meléndez,[3] B. Gustafsson,[4,5] L. M. Howes,[1,6] I. U. Roederer,[7] D. L. Lambert[2] and T. Bensby[6]

[1]*Research School of Astronomy and Astrophysics, Australian National University, Canberra, ACT 2611, Australia*
[2]*McDonald Observatory and Department of Astronomy, University of Texas at Austin, 2515 Speedway, Austin, TX 78712-1205, USA*
[3]*Departamento de Astronomia do IAG/USP, Universidade de Sao Paulo, Rua do Matao 1226, Sao Paulo 05508-900, SP, Brasil*
[4]*Institution for Physics and Astronomy, Uppsala University, Box 515, SE-75120 Uppsala, Sweden*
[5]*Nordita, Roslagstullsbacken 23, SE-10691 Stockholm, Sweden*
[6]*Lund Observatory, Department of Astronomy and Theoretical physics, Lund University, Box 43, SE-22100 Lund, Sweden*
[7]*Department of Astronomy, University of Michigan, 1085 South University Avenue, Ann Arbor, MI 48109, USA*

Accepted 2015 November 29. Received 2015 November 27; in original form 2015 April 16

ABSTRACT

Chemical abundance studies of the Sun and solar twins have demonstrated that the solar composition of refractory elements is depleted when compared to volatile elements, which could be due to the formation of terrestrial planets. In order to further examine this scenario, we conducted a line-by-line differential chemical abundance analysis of the terrestrial planet host Kepler-10 and 14 of its stellar twins. Stellar parameters and elemental abundances of Kepler-10 and its stellar twins were obtained with very high precision using a strictly differential analysis of high quality Canada–France–Hawaii Telescope, Hobby–Eberly Telescope and Magellan spectra. When compared to the majority of thick disc twins, Kepler-10 shows a depletion in the refractory elements relative to the volatile elements, which could be due to the formation of terrestrial planets in the Kepler-10 system. The average abundance pattern corresponds to ∼13 Earth masses, while the two known planets in Kepler-10 system have a combined ∼20 Earth masses. For two of the eight thick disc twins, however, no depletion patterns are found. Although our results demonstrate that several factors [e.g. planet signature, stellar age, stellar birth location and Galactic chemical evolution (GCE)] could lead to or affect abundance trends with condensation temperature, we find that the trends give further support for the planetary signature hypothesis.

Key words: planets and satellites: formation – planets and satellites: terrestrial planets – stars: abundances – stars: individual: Kepler-10.

1 INTRODUCTION

The technique of a strictly differential line-by-line analysis for measuring relative chemical abundances in stars with very high precision (0.01 dex, ∼2 per cent) has been further developed and applied to various cases over the past few years (Meléndez et al. 2009, 2012; Ramírez et al. 2011, 2014; Yong et al. 2013; Liu et al. 2014; Tucci Maia, Meléndez & Ramírez 2014; Biazzo et al. 2015; Nissen 2015; Saffe, Flores & Buccino 2015). This unprecedented precision has revealed subtle chemical differences in the photospheres of stars which have been interpreted as a signature of planet formation. Meléndez et al. (2009) demonstrated that the Sun exhibits a peculiar chemical pattern when compared to solar twins, namely, a depletion of refractory elements relative to volatile elements. They tentatively attributed this pattern to the formation of planets, especially rocky planets, in the Solar system. In their scenario, refractory elements in the proto-solar nebula were locked up in the terrestrial planets. The remaining dust-cleansed gas was then accreted on to the Sun. In contrast, the typical solar twin did not form terrestrial planets efficiently, or dumped their proto-planetary nebulae, cleansed from refractories by planetary formation, so early that the stellar convection was still deep enough to dilute the disc gas to erase its chemical signature. Therefore, the Sun would exhibit a depletion in refractory elements relative to volatile elements when compared to most solar twins. Chambers (2010) confirm quantitatively that the depletion of refractories in the solar photosphere is possibly due to the depletion of a few Earth masses of rocky material.

★ Based on observations obtained at the 3.6m Canada–France–Hawaii Telescope located at the Mauna Kea Observatory, US, the 9.2 m Hobby–Eberly Telescope located at the W.J. McDonald Observatory of the University of Texas at Austin, US, and the 6.5 m Magellan Clay Telescope located at the Las Campanas Observatory, Chile.

† E-mail: fan.liu@anu.edu.au

This scenario, however, has been challenged by González Hernández et al. (2010) and Adibekyan et al. (2014). They argued that the observed trend between chemical abundances and condensation temperature (T_c) could possibly be due to the differences in stellar ages rather than the presence of planets. Nissen (2015) conducted a high-precision differential abundance analysis for 21 solar twin stars in the solar neighbourhood with high signal-to-noise ratio (SNR > 600) spectra. His results revealed abundance–age correlations for most elements. This indicates that chemical evolution in the Galactic disc might play an important role in the explanation of the trend between abundance and dust condensation temperature and must be considered when interpreting the results.

Another explanation for the peculiar solar composition is that the pre-solar nebula was radiatively cleansed from some of its dust by luminous hot stars in the solar neighbourhood before the formation of the Sun and its planets. This possibility is supported by the finding that the solar-age and rich open cluster M67 seems to have a chemical composition closer to the solar composition than most solar twins (Önehag et al. 2011; Önehag, Gustafsson & Korn 2014). A similar scenario was discussed by Gaidos (2015), who suggests that abundance–T_c correlations could be explained by dust–gas segregation in circumstellar discs.

The scenario put forward by Meléndez et al. (2009) makes a testable prediction that the host star of a system with terrestrial planets should also exhibit a depletion in refractory elements relative to volatile elements when compared to otherwise identical stars (i.e. stellar parameters, ages, birth locations). Therefore, in order to test this scenario, we need to conduct high-precision chemical abundance studies of stars hosting terrestrial planets relative to similar other stars without such planets. Kepler-10 hosts two planets, Kepler-10b and Kepler-10c (Batalha et al. 2011). Dumusque et al. (2014) reported that the mass of Kepler-10b is 3.33 ± 0.49 $M_\oplus$ with a density of 5.8 ± 0.8 g cm^{-3}, while the mass of Kepler-10c is 17.2 ± 1.9 $M_\oplus$ with a density of 7.1 ± 1.0 g cm^{-3}. Dumusque et al. (2014) characterized Kepler-10b and Kepler-10c as a hot Earth-like planet and a Neptune mass solid planet, respectively, although Rogers (2015) argued that Kepler-10c is likely to have a substantial volatile envelope and thus not rocky. The Kepler-10 system is thus a very suitable target to identify any chemical signatures of terrestrial planet formation. In particular, if the scenario presented by Meléndez et al. (2009) is correct, we should expect to find a deficiency of refractory elements relative to volatile elements in the photosphere of Kepler-10 when compared to other stars sharing similar stellar parameters but without known planets.

Here, we present a strictly line-by-line differential abundance analysis of Kepler-10 and a sample of stellar twins to explore whether or not there is a chemical signature of terrestrial planet formation.

2 OBSERVATIONS AND DATA REDUCTION

We obtained high resolution and high SNR spectra with the Canada–France–Hawaii Telescope (CFHT), the Hobby–Eberly Telescope (HET) and the Magellan Clay Telescope.

We observed Kepler-10 with the Echelle SpectroPolarimetric Device for the Observation of Stars (Manset & Donati 2003) at the CFHT during 2013 June. The spectral revolving power is 68 000 and the spectral range is 3800–8900 Å. In total eight spectra with exposures of 1700 s each were obtained. The individual frames were combined into a single spectrum with SNR ≈ 300 per pixel in most wavelength regions. A solar spectrum with even higher SNR (≈500 per pixel) was obtained by observing the asteroid Vesta. The spectra were reduced with the CFHT data reduction tool 'LIBRE-ESPIRIT' while the continuum normalizations were addressed with IRAF.[1]

We also observed Kepler-10 with the High Resolution Spectrograph (HRS; Tull 1998) on the HET at McDonald Observatory during 2011 May. A total integration time of 6.8 h was needed to achieve SNR > 350 per pixel. The spectrum has a spectral resolving power of 60 000 and covers 4100–7800 Å, with a gap of about 100 Å around 6000 Å. A solar spectrum with higher spectral resolution ($R = 120\,000$) and higher SNR (≈500 per pixel) was obtained by observing the asteroid Iris. The HRS-HET data were reduced using IRAF's ECHELLE package.

We selected 14 stars identified as Kepler-10 stellar twins, based on the similarity of their stellar parameters ($T_{\rm eff}$, $\log g$, [Fe/H]) to those of Kepler-10, using an updated version of the stellar parameter catalogue of Ramírez & Meléndez (2005) and from the sample by Bensby, Feltzing & Oey (2014). The comparison star sample was chosen randomly such that any individual star was not necessarily included in planet search programmes. Those 'Kepler-10 twins' were observed using the Magellan Inamori Kyocera Echelle spectrograph (Bernstein et al. 2003) during two runs: 2014 June and 2015 June. The spectrograph delivers wavelength coverage from about 3300 to 5000 Å (blue arm) and 4900 to 9400 Å (red arm) at a spectral resolving power of 83 000 and 65 000, respectively, the SNR exceeded 300 per pixel at 6000 Å. A solar spectrum using the asteroid Vesta was obtained each night in the first run. We reduced the spectra with standard procedures which include bias subtraction, flat-fielding, scattered-light subtraction, 1D spectral extraction, wavelength calibration and continuum normalization, with IRAF.

Our thick disc twins were not observed with the northern telescopes, nor was it possible to observe Kepler-10 from the southern Magellan site. This limits our strictly differential study to the use of the solar-spectrum observations as a test calibration. We also carried out a number of tests which ensure that our results are not compromised by the use of different spectroscope/telescope combinations. The most important of these tests are described later in this paper.

3 STELLAR ATMOSPHERIC PARAMETERS

The line list employed in our analysis was adopted mainly from Asplund et al. (2009) and complemented with additional unblended lines from Bensby et al. (2005) and Neves et al. (2009); in a differential abundance analysis the accuracy of the *gf* values does not influence the results. Equivalent widths (EWs) were measured using the ARES code (Sousa et al. 2007) for most lines. The EWs for C, O, Mg, Al, S, Mn, Cu and Zn (i.e. elements with fewer lines) were measured manually with the SPLOT task in IRAF. Weak (<5 mÅ) and strong (>110 mÅ) lines were excluded from the analysis. The atomic line data adopted for the abundance analysis are listed in Table A1. We emphasize that in a differential analysis such as ours, the atomic data have essentially no influence on the results since Kepler-10 and its twins have very similar stellar parameters.

We performed a 1D, local thermodynamic equilibrium (LTE) abundance analysis using the 2013 version of MOOG (Sneden 1973; Sobeck et al. 2011) with the ODFNEW grid of Kurucz model atmospheres (Castelli & Kurucz 2003). Stellar parameters were obtained by forcing excitation and ionization balance of Fe I and Fe II lines

[1] IRAF is distributed by the National Optical Astronomy Observatory, which is operated by Association of Universities for Research in Astronomy, Inc., under cooperative agreement with National Science Foundation.

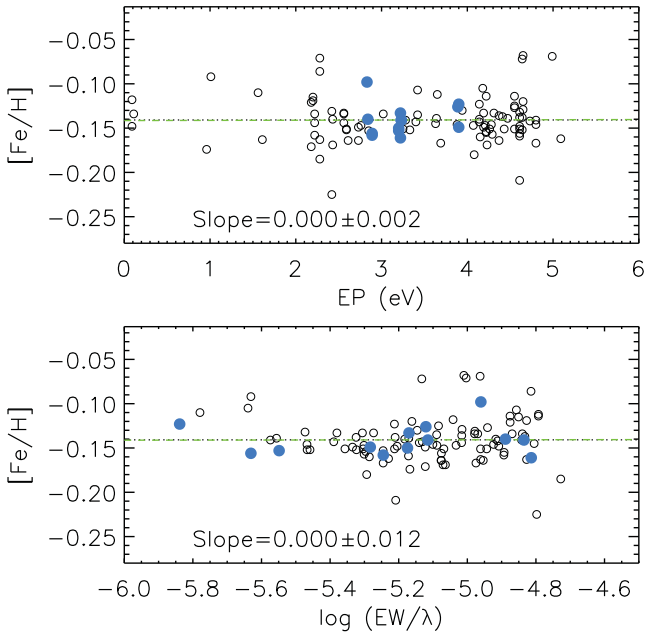

Figure 1. Top panel: [Fe/H] of Kepler-10 derived on a line-by-line basis with respect to the Sun as a function of lower EP; open circles and blue-filled circles represent Fe I and Fe II lines, respectively. The black dotted line shows the location of mean [Fe/H], the green dashed line represents the best fit to the data. Bottom panel: same as in the top panel but as a function of reduced EW.

on a line-by-line basis relative to the Sun. The adopted parameters for the Sun were $T_{\rm eff} = 5777$ K, $\log g = 4.44$, [Fe/H] = 0.00, $\xi_{\rm t} = 1.00$ km s^{-1}. The stellar parameters of Kepler-10 and its stellar twins were established separately using an automatic grid searching method described by Liu et al. (2014). The best combination of $T_{\rm eff}$, $\log g$, [Fe/H] and $\xi_{\rm t}$, minimizing the slopes in [Fe I/H] versus excitation potential (EP) and reduced EW as well as the difference between [Fe I/H] and [Fe II/H], is obtained from a successively refined grid of stellar atmospheric models. The final solution was obtained when the grid step-size decreased to $\Delta T_{\rm eff} = 1$ K, $\Delta \log g = 0.01$ and $\Delta \xi_{\rm t} = 0.01$ km s^{-1}. We also required the derived average [Fe/H] to be consistent with the adopted model atmospheric value. Lines whose abundances departed from the average by $>2.5\sigma$ were clipped.

Fig. 1 shows an example of determining the stellar parameters of Kepler-10. The adopted stellar parameters satisfy the excitation and ionization balance in a differential sense. The best-fitting $\pm 1\sigma$ for the [Fe/H] versus EP roughly corresponds to an error in $T_{\rm eff}$ of 10 K, similarly for the reduced EW [log (EW/λ)], which corresponds to an error of ∼0.02–0.03 km s^{-1} in $\xi_{\rm t}$. The abundance difference in Fe I and Fe II = 0.000 ± 0.006, which constrains $\log g$ to a precision of 0.02–0.03.

For the 14 stellar twins, differential stellar parameters were also obtained by the line-by-line differential analysis as described before, but relative to Kepler-10 rather than the Sun, i.e. Stellar twins (Magellan) − Kepler-10 (HET or CFHT). The adopted initial parameters for Kepler-10 were $T_{\rm eff} = 5700$ K, $\log g = 4.35$, [Fe/H] = −0.15, $\xi_{\rm t} = 1.00$ km s^{-1}, taken from the Kepler-10 analysis relative to the Sun. We emphasize that the absolute values are not crucial for our differential abundance analysis. We did not consider α enhancements in the thick disc stars in the model atmospheres but this does not affect our results, in particular not in the differential study of Kepler-10 relative to its thick disc twins. We assume that the stellar spectrum is defined solely by the stellar parameters $T_{\rm eff}$, $\log g$, $\xi_{\rm t}$ and abundances, i.e. other individual stellar parameters, e.g. describing stellar activity is not considered in this study.

The final adopted atmospheric parameters of Kepler-10 and its stellar twins are listed in Table 1. The uncertainties in the stellar parameters were derived with the method described by Epstein et al. (2010) and Bensby et al. (2014), which accounts for the covariances between changes in the stellar parameters and the differential abundances. Excellent precision was achieved due to the strictly differential method, which should greatly reduce the systematic errors from atomic line data and shortcomings in the 1D LTE modelling of the stellar atmospheres and spectral line formation (e.g. Asplund 2005).

4 RESULTS

4.1 Elemental abundances

Having established the stellar parameters for Kepler-10 and its stellar twins, we derived chemical abundances relative to the Sun for an additional 17 elements from atomic lines: C, O, Na, Mg, Al, Si, S, Ca, Sc, Ti, V, Cr, Mn, Co, Ni, Cu and Zn. We also obtained differential abundances of Kepler-10's stellar twins relative to Kepler-10. Hyperfine-structure splitting was considered for Sc, V, Cr, Mn and Cu using data from Kurucz & Bell (1995). Departures from LTE were considered for the 777 nm oxygen triplet lines according to Ramírez, Allende Prieto & Lambert (2007) and the typical size of the correction is ≈ −0.01 dex. The errors in the differential abundances were calculated following the method of Epstein et al. (2010): the standard errors in the mean abundances, as derived from the different spectral lines, were added in quadrature to the errors introduced by the uncertainties in the atmospheric parameters. Most derived elemental abundances have uncertainties ≤0.02 dex, which further underscores the advantages of a strictly differential analysis. Indeed, when considering all elements, the average uncertainty is only 0.014 ± 0.002 ($\sigma = 0.006$) for Kepler-10 relative to the Sun.

We first compare the abundances of Kepler-10 as derived from HET and CFHT spectra (Fig. 2). The values of $T_{\rm c}$ (specifically 50 per cent condensation temperature for a solar-composition mixture) are given by Lodders (2003). The average abundance difference Δ[X/H] (HET − CFHT) is −0.004 ± 0.005 ($\sigma = 0.021$), consistent with zero. We perform a least-squares linear fit weighted by the errors in abundances while the uncertainties of the fitting are calculated considering the chi-square merit function and the relative derivatives.[2] We note that there is a slight negative trend between Δ[X/H] versus $T_{\rm c}$ with a slope of $(-0.19 \pm 0.09) \times 10^{-4}$ K^{-1}, which is mainly driven by the two volatile elements, C and O. We adopt the results derived from the HET spectra. This choice does not affect our conclusions since the differences between HET and CFHT data are very small. We do explore the effects of using CFHT data below.

Another issue regarding systematic offsets that we need to consider carefully is whether the choice of the spectrograph affects the results. According to Bedell et al. (2014), systematic offsets may be introduced when comparing the results using spectra obtained from different instruments or when measurements are not performed consistently. While the Kepler-10 differential abundances were measured based on HET spectra, differential abundances for

[2] We applied the same manner to all the following linear fits.

Table 1. Stellar parameters of Kepler-10 and its stellar twins.

Object	$T_{\rm eff}$ (K)	log g	$\xi_{\rm t}$ (km s^{-1})	[Fe/H]	Probability[a] Thin disc (per cent)	Probability[a] Thick disc (per cent)	Population	Age (Gyr)
Kepler-10[b]	5697 ± 10	4.40 ± 0.03	0.98 ± 0.02	−0.141 ± 0.009	3	96	thick	8.4 ± 1.0
Kepler-10[c]	5695 ± 13	4.38 ± 0.04	0.96 ± 0.03	−0.143 ± 0.015	3	96	thick	9.0 ± 1.1
HD 88084[d]	5780 ± 13	4.40 ± 0.03	1.05 ± 0.03	−0.091 ± 0.012	98	2	thin	5.8 ± 1.4
HD 115382[d]	5776 ± 12	4.38 ± 0.03	1.05 ± 0.03	−0.089 ± 0.010	92	8	thin	6.7 ± 1.4
HD 126525[d]	5687 ± 19	4.50 ± 0.03	1.00 ± 0.04	−0.063 ± 0.014	91	9	thin	2.6 ± 1.5
HD 117939[d]	5729 ± 13	4.45 ± 0.03	1.00 ± 0.03	−0.176 ± 0.016	60	40	thin	4.7 ± 1.5
HIP 113113[d]	5706 ± 13	4.42 ± 0.04	0.96 ± 0.03	−0.071 ± 0.012	58	42	thin	5.6 ± 1.6
HD 117126[d]	5779 ± 18	4.25 ± 0.04	1.10 ± 0.03	−0.032 ± 0.015	55	44	thick	8.2 ± 0.5
HD 115231[d]	5708 ± 15	4.43 ± 0.04	1.00 ± 0.04	−0.095 ± 0.015	38	61	thick	5.8 ± 1.6
HD 106210[d]	5701 ± 13	4.40 ± 0.04	0.96 ± 0.03	−0.131 ± 0.014	18	80	thick	7.0 ± 1.6
HIP 109821[d]	5772 ± 14	4.32 ± 0.03	1.06 ± 0.03	−0.087 ± 0.011	17	82	thick	7.7 ± 0.8
HD 87320[d]	5666 ± 12	4.40 ± 0.03	0.93 ± 0.03	−0.149 ± 0.010	11	87	thick	7.5 ± 1.4
HIP 96124[d]	5636 ± 13	4.41 ± 0.04	0.93 ± 0.03	−0.197 ± 0.012	9	90	thick	8.2 ± 1.6
HIP 101857[d]	5798 ± 14	4.34 ± 0.03	1.06 ± 0.03	+0.029 ± 0.012	2	96	thin[e]	6.4 ± 0.8
HIP 9381[d]	5734 ± 14	4.39 ± 0.04	1.02 ± 0.03	−0.238 ± 0.012	1	96	thick	8.0 ± 1.7
HIP 99224[d]	5754 ± 18	4.27 ± 0.04	1.03 ± 0.04	−0.004 ± 0.014	0	96	thick	8.2 ± 0.6

Notes. [a]Probabilities calculated based on kinematics (Ramírez, Allende Prieto & Lambert 2013).
[b]Parameters derived with HET data.
[c]Parameters derived with CFHT data.
[d]Parameters derived using Kepler-10 (HET) as the reference.
[e]HIP 101857 is assigned to the thin disc because of its abundance pattern rather than kinematics.

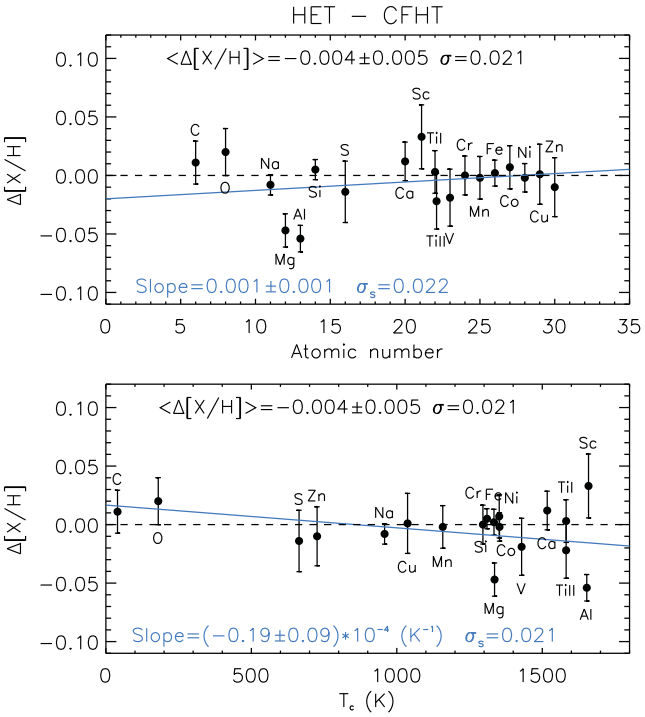

Figure 2. Top panel: abundance differences for Kepler-10 from two different telescopes, Δ[X/H] (HET − CFHT), versus atomic number; the blue solid line represents the linear fit to the data; σ_s is the dispersion about the linear fit. Bottom panel: abundance differences as a function of condensation temperature $T_{\rm c}$.

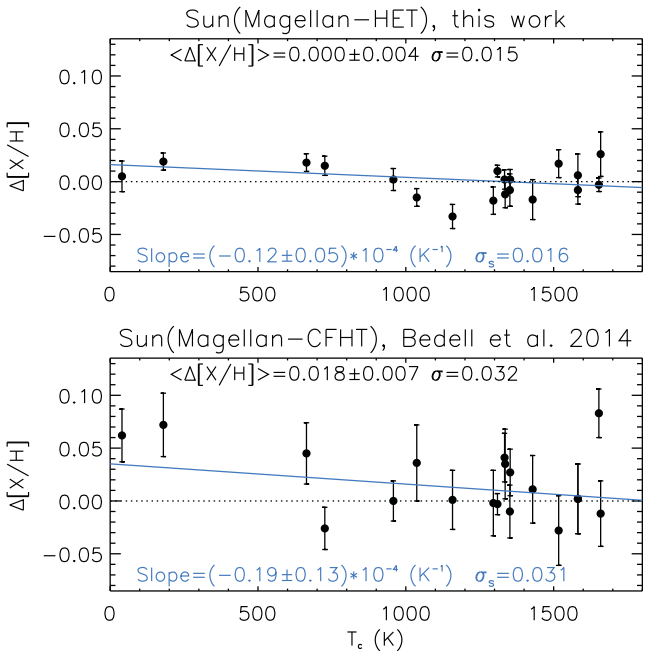

Figure 3. Abundance differences Δ[X/H] versus condensation temperature $T_{\rm c}$ for solar spectra obtained with different instruments (Magellan − HET) for this work (top panel) and for Bedell et al. (2014) (Magellan − CFHT) (bottom panel). The blue solid lines represent the linear fit to our data (top panel) and the Bedell et al. (2014) data (bottom panel), σ_s is the dispersion about the linear fit.

the Kepler-10 stellar twins were measured based on Magellan spectra. Therefore, it is crucial to check whether any systematic offsets exist. In Fig. 3, we plot Δ[X/H] as a function of $T_{\rm c}$ derived from solar spectra obtained with different instruments [Sun (Magellan − HET)]. In that figure, we also include a comparison of the Sun (Magellan − CFHT) from Bedell et al. (2014). The average difference in our Δ[X/H] is 0.000 ± 0.004 (σ = 0.015) and the slope of the linear fit is (−0.12 ± 0.05) × 10^{-4} K^{-1}. The systematic offsets in our work are much smaller than that in Bedell et al. (2014). One possible reason for this difference is that in Bedell et al. (2014), the normalization of spectra and the measurement of EWs involved

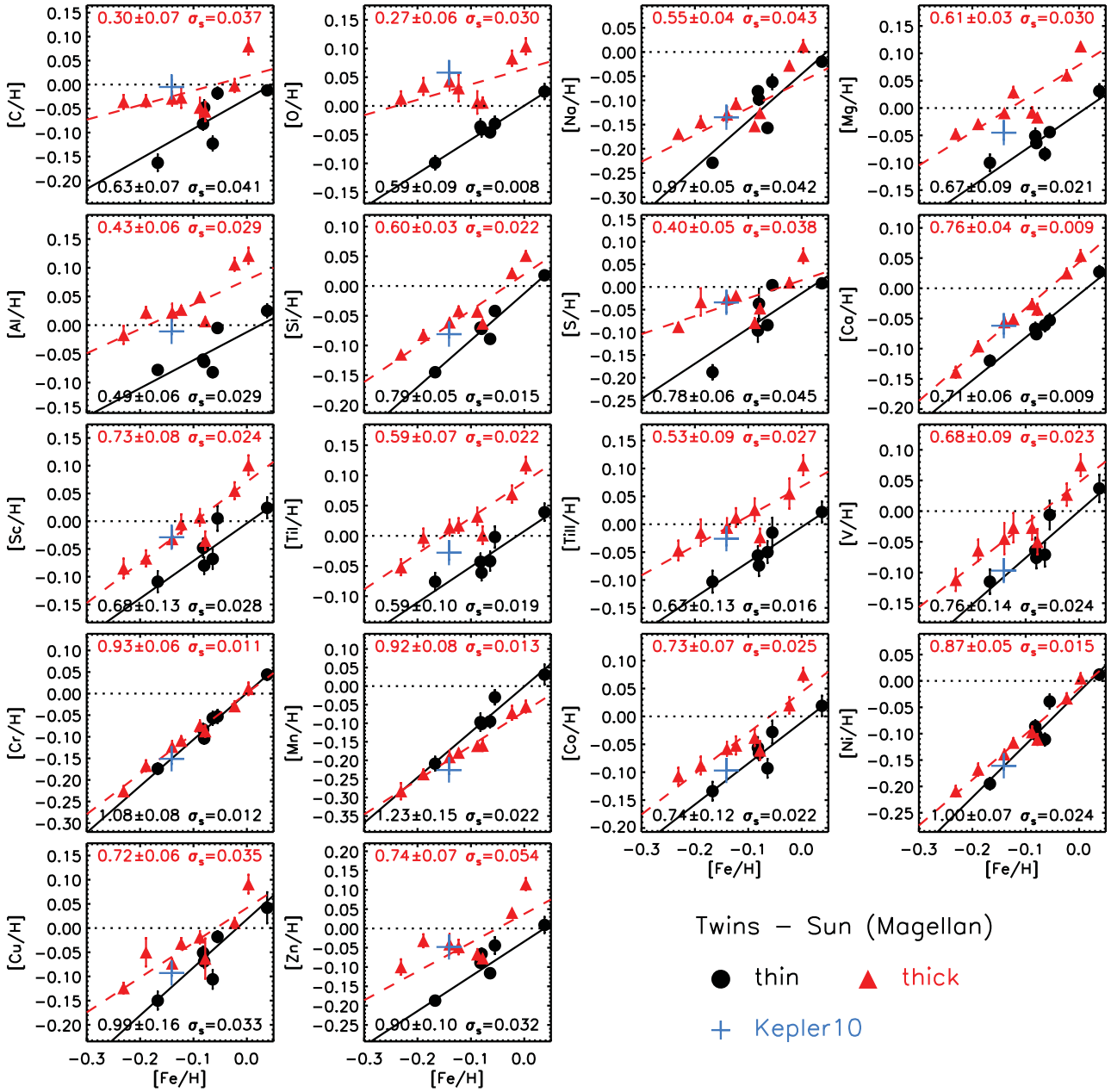

Figure 4. [X/H] versus [Fe/H] for various elements for the 'Kepler-10 twins' [Twins − Sun (Magellan)]. Linear fits for the thin disc counterparts (black circles) and thick disc (red triangles) twins are overplotted, σ_s is the dispersion about the linear fit. The location of Kepler-10 is marked [Kepler-10 − Sun (HET), blue crosses]. The size of the crosses are corresponding to the error bars in [X/H] and [Fe/H].

not only different instruments, but also different investigators. In this work, the entire analysis was done consistently by one person using the same approach, minimizing the possible systematic errors introduced by comparing the results based on different instruments.

The discovery paper by Batalha et al. (2011) reported [Fe/H] = -0.15 ± 0.04 for Kepler-10. We confirm that Kepler-10, with [Fe/H] = -0.141 ± 0.009, is metal-poor relative to the Sun.[3] Kepler-10 is also older than the Sun with an age of 8.4 ± 1.0 Gyr from our derivation, see below. The total space velocity [$V_{\rm tot} = (U^2 + V^2 + W^2)^{1/2}$] of Kepler-10 is 97.0 km s^{-1} and the kinematic probability of being from the thick disc is 96 per cent (Dumusque et al. 2014). Therefore, direct comparisons of Kepler-10 to the Sun is not adequate. Kepler-10 should be compared against stars of similar metallicity and belonging to the same stellar population. For the 14 Kepler-10 stellar twins without known planets, we show the distribution in [Fe/H] and [X/H] in Fig. 4. We calculated the Galactic space velocities U, V, W of our sample stars using data from SIMBAD data base with the equations given by e.g. Johnson & Soderblom (1987). We derived the associated probabilities of thin/thick disc membership based on the algorithm described by Ramírez et al. (2007, 2013). We computed the stellar ages using the stellar parameters and their errors as given in Table 1, placing them on a $T_{\rm eff}$–log g plane, and comparing these locations with the theoretical isochrones of the Yonsei–Yale group (e.g. Yi et al. 2001;

[3] Recently, a very similar metallicity of [Fe/H] = -0.14 ± 0.02 was presented by Santos et al. (2015).

Kim et al. 2002). Details of our age determination technique are provided in Ramírez et al. (2014).

We have three criteria for thick disc membership: kinematic probability >60 per cent, age > 7 Gyr and chemical similarity with thick disc stars. All the eight thick disc twins fulfil at least two of these criteria (see Table 1). The remaining programme stars are likely thin disc members. Regarding the latter criterion, it is evident from Fig. 4 (and previous work by Reddy, Lambert & Allende Prieto 2006; Bensby et al. 2014) that thin and thick disc stars lie on different and well-defined trends, although there are also some objects that exhibit thick disc kinematics but thin disc abundances (Reddy et al. 2006). In the present work, we are searching for subtle chemical abundance differences among thick disc stars, so it is important that these comparison stars have thick disc chemical abundances.

4.2 Δ[X/H]–T_c correlations

The [X/H] ratios confirm that Kepler-10 is a thick disc object and its relatively old age further supports this. Therefore, we will compare Kepler-10 against its thick disc stellar twins in order to compensate for effects of Galactic chemical evolution (GCE). As is seen directly from Fig. 4, the abundances of Kepler-10 show a systematical pattern relative to the linear fits in the panel that presumably display the GCE as relations between [X/H] and [Fe/H]. E.g., for the five elements with the lowest condensation temperatures, C, O, S, Zn and Na, the blue crosses representing Kepler-10 in the panels of the figure are situated on or above the redline, while for the eight elements with the highest condensation temperature, Mg, Co, Ni, V, Ca, Ti, Al and Sc, Kepler-10 is located on or below the redline. It is easy to demonstrate that if we assume that the real abundances of Kepler-10 would be on the line and the observed locations are reflecting independent errors symmetrically distributed (i.e. with equally probable departures in positive or negative directions), the chance of obtaining this systematic effect with T_c by mere chance is less than 1 per cent. In view of the fact that the present study was initiated when the super-Earths of Kepler-10 had been discovered in order to test the planetary signature of the abundance–T_c relation, the systematics of Fig. 4 is in itself a striking confirmation, indicating that this interpretation must be favoured relative to e.g. chemical evolution effects.

To improve the precision further, we derive strictly differential abundances Δ[X/H] for the eight likely thick disc stellar twins relative to Kepler-10 in Fig. 5 rather than relative to the Sun as the case for Fig. 4. We find that a single linear fit provides an appropriate representation of the Δ[X/H]–T_c correlation when comparing the thick disc twins to Kepler-10. Our results demonstrate that the Δ[X/H]–T_c trends could vary from star to star, as reported by Nissen (2015). Five stars (HIP 109821, HIP 99224, HD 106210, HD 115231 and HD 117126) show positive slopes for the single linear fitting but the trends are driven mainly by the abundances of the most volatile elements C and O. HD 87320 shows a positive slope as well but with much larger scatter around the best fit. HIP 9381 and HIP 96124 show large scatters around the zero-slopes with three elements as outliers (Cr, Mn and Fe). These outlier elements could be due to the impact of GCE since these two stars are the most metal-poor and those three elements (Cr, Mn and Fe) exhibit the steepest slopes for the [X/H] versus [Fe/H] in Fig. 4.

We average the results of the differential abundances Δ[X/H] for these eight thick disc stellar twins [i.e. ⟨thick disc twins (Magellan)⟩ − Kepler-10 (HET)] and show the result in Fig. 6. As seen already directly from Fig. 4, Kepler-10 shows a depletion of refractory elements relative to the volatile elements when compared to the average of all the thick disc stellar twins. The average difference is $\Delta[X/H] = 0.037 \pm 0.004$ ($\sigma = 0.016$). A linear fit to the data has a gradient of $(0.29 \pm 0.03) \times 10^{-4}$ K^{-1}, corresponding to a $>9\sigma$ significance. Although the trend is mainly driven by C and O, a significant trend [slope $= (0.17 \pm 0.04) \times 10^{-4}$ K^{-1}] is also present when excluding these two elements. Table 2 lists the adopted elemental abundances and associated uncertainties of Kepler-10 and the average of its thick disc stellar twins. In addition, Table A2 lists all the derived elemental abundances and associated uncertainties of each programme star with relative to Kepler-10.

Although the classification of Kepler-10 as a thick disc star, on the basis of its kinematics, age and abundance pattern, one may ask how the abundance pattern relative to T_c would look if compared with its thin disc counterpart stars, instead. In Fig. 7, we display the differences between the mean of [X/H] for the thin disc stars and Kepler-10, again plotted versus T_c. A linear fit to the data has a gradient of $(0.45 \pm 0.03) \times 10^{-4}$ K^{-1}, while the dispersion about the linear fit (σ_s) is 0.044 dex. The trend excluding C and O has a gradient to be $(-0.12 \pm 0.04) \times 10^{-4}$ K^{-1} with 2.6σ significance. We see that the systematic slope of the relation still prevails, but that it is now very much dependent on C and O; the relation for the rest of the elements show a characteristic peak, corresponding to elements with $T_c \sim 1200$ K. This demonstrates that GCE partly masks the effects of dust-depletion on the abundance pattern.

As a further check of our results, we also repeated the analysis using the CFHT Kepler-10 spectrum and analysed the stellar twins with respect to that spectrum. The results are very similar to those presented in Figs 5–7.

5 DISCUSSION

As shown in Fig. 6, there is a deficiency of refractory elements relative to volatile elements in the photosphere of the terrestrial planet host Kepler-10 when compared to the average results of its thick disc stellar twins without known planets. Using the current size of the convective zone of Kepler-10 (0.08 $M_\odot$; Siess, Dufour & Forestini 2000), the abundance pattern corresponds to at least 13 Earth masses of rocky material (Chambers 2010) which is comparable to the total mass of planets (20 Earth masses) in the Kepler-10 system. Therefore, the differences in chemical composition between Kepler-10 and its thick disc stellar twins could be attributed to the formation of terrestrial planets in the Kepler-10 system, but this requires that the lifetime of the proto-planetary disc was long enough to not deliver its dust-cleansed gas until the convection zone of the star reached its present depth. As we mentioned before, even for the thick disc twins which share similar stellar parameters and ages with Kepler-10, the Δ[X/H]–T_c correlations still vary star to star. In order to investigate this further, we show the histogram of the slopes for the single linear fitting of the T_c trends for the eight thick disc stars in Fig. 8. The slopes exhibit a broad distribution. We note that two (HIP 9381 and HIP 96124) of the thick disc stars do not show any apparent trends, which complicates the scenario of the chemical signatures of terrestrial planets. If the Δ[X/H]–T_c trends do reflect planet formation, those two stars could be conjectured to also harbour terrestrial planets that have not yet been detected. The first one (HIP 9381) has been observed multiple times with HARPS yet no results have been published. It is also probable that other factors play a role in determining the detailed chemical composition of those stars.

Adibekyan et al. (2014) and Nissen (2015) proposed that the trends between chemical abundance and condensation temperature (T_c) could be due to the differences in the stellar ages. We plot

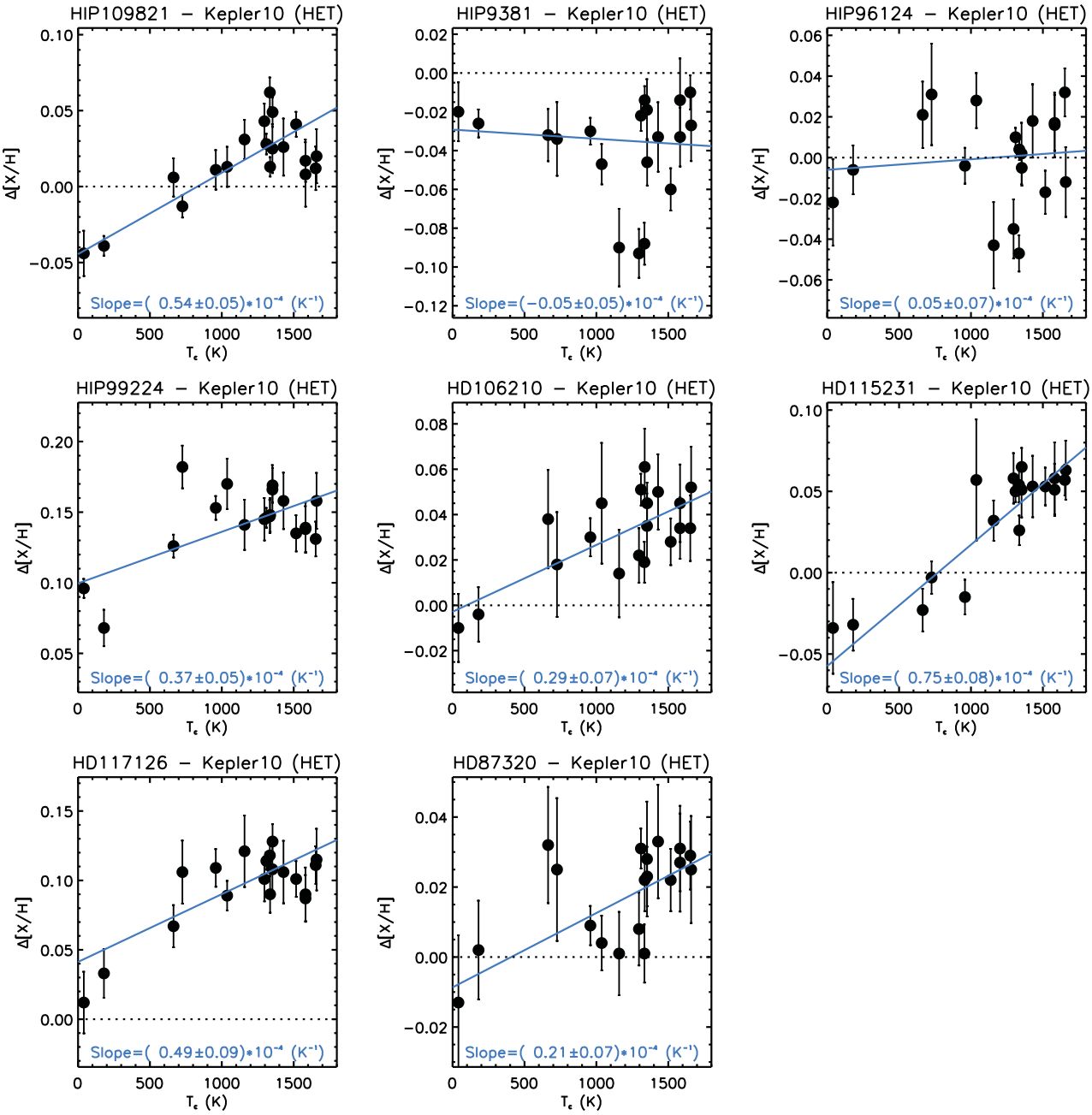

Figure 5. Abundance differences Δ[X/H] versus condensation temperature T_c for all the thick disc stellar twins relative to Kepler-10. The blue solid lines show the single linear fit to the results.

the differential abundances Δ[X/H]–T_c slopes versus stellar ages in Fig. 9. A linear fit to the data is overplotted (each data point is given equal weight). The gradient is -1.8 ± 1.0 for thick disc twins, using Kepler-10 as a reference. The negative slope is likely driven by the one star younger than 6 Gyr. Without that object, the diagram is a scatter plot such that age alone cannot explain the chemical behaviour. We note that for most thick disc twins, although they have similar ages, the Δ[X/H]–T_c slopes can vary by $\sim 6 \times 10^{-5}$ K^{-1}. Therefore, we emphasize again that age alone cannot explain the chemical patterns found in Figs 5 and 6.

It has since long been known that the solar upper atmosphere and wind abundances are affected by anomalies, with respect to the photosphere, in that the elements with a high first ionization potential (FIP; such as Ne and Ar) are depleted relative to those with low potentials (e.g. Fe, Mg, Si, see Feldman & Laming 2000). Effects of this kind could possibly occur differentially in stellar photospheres, and might mimic the abundance correlations with condensation temperature. We have explored this by examining the relation between Δ[X/H] and the FIP in Fig. 10. Although a correlation is apparent, its significance (4σ) is much less than for the T_c trend. Fig. 10 might be just as well considered as providing two clumps: C and O, the rest of the elements, respectively. A similar phenomenon was also reported by Ramírez et al. (2010) for the Meléndez et al. (2009) and Ramírez, Meléndez & Asplund (2009) solar twin data sets. We performed a Spearman correlation test of the abundance differences versus T_c and FIP. The Spearman correlation

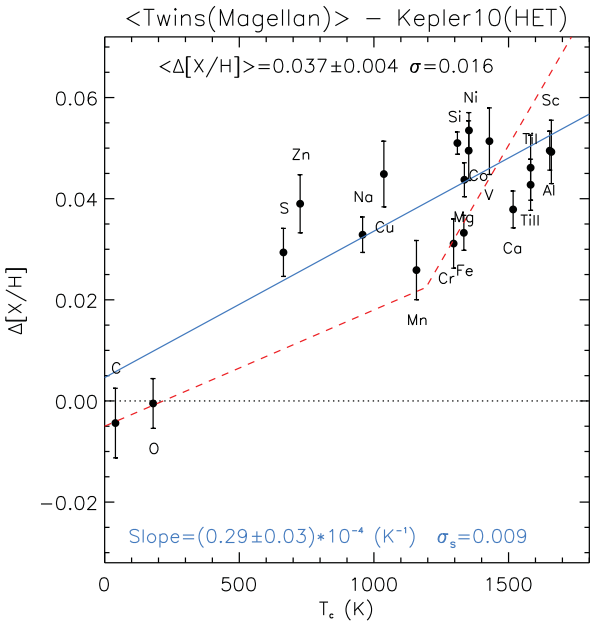

Figure 6. Average abundance differences Δ[X/H] versus condensation temperature T_c for the eight thick disc stellar twins relative to Kepler-10. The blue solid line represents the linear fit to the data, σ_s is the dispersion about the linear fit and the red dashed line is the fit from Meléndez et al. (2009) for solar twins − Sun, normalized to Δ[C/H].

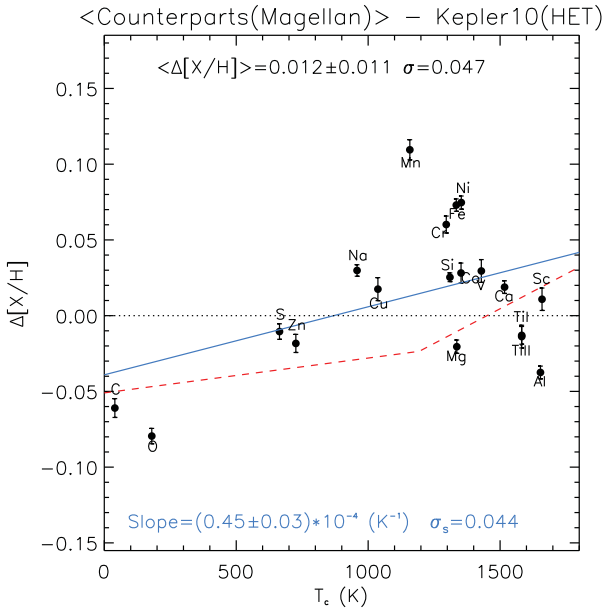

Figure 7. Average abundance differences Δ[X/H] versus condensation temperature T_c for the thin disc counterparts relative to Kepler-10. The blue solid line represents the linear fit to the data, σ_s is the dispersion about the linear fit and the red dashed line is the fit from Meléndez et al. (2009) for solar twins − Sun.

Table 2. [X/H] for Kepler-10 and the average of its thick disc stellar twins.

Element	Kepler-10[a]	Kepler-10[b]	⟨Thick disc twins⟩[c]
C	−0.005 ± 0.015	−0.016 ± 0.011	−0.004 ± 0.006
O	0.058 ± 0.010	0.038 ± 0.017	−0.001 ± 0.005
Na	−0.135 ± 0.007	−0.127 ± 0.005	0.033 ± 0.003
Mg	−0.045 ± 0.013	0.002 ± 0.006	0.044 ± 0.004
Al	−0.011 ± 0.005	0.043 ± 0.010	0.050 ± 0.004
Si	−0.081 ± 0.006	−0.086 ± 0.006	0.051 ± 0.002
S	−0.034 ± 0.022	−0.020 ± 0.014	0.029 ± 0.005
Ca	−0.062 ± 0.013	−0.074 ± 0.010	0.038 ± 0.004
Sc	−0.029 ± 0.018	−0.062 ± 0.020	0.049 ± 0.006
Ti I	−0.028 ± 0.012	−0.031 ± 0.014	0.043 ± 0.005
Ti II	−0.026 ± 0.012	−0.004 ± 0.021	0.046 ± 0.006
V	−0.097 ± 0.016	−0.078 ± 0.018	0.051 ± 0.007
Cr	−0.151 ± 0.012	−0.151 ± 0.011	0.031 ± 0.005
Mn	−0.226 ± 0.011	−0.224 ± 0.015	0.026 ± 0.006
Fe	−0.141 ± 0.009	−0.143 ± 0.015	0.033 ± 0.003
Co	−0.097 ± 0.013	−0.104 ± 0.013	0.050 ± 0.006
Ni	−0.161 ± 0.007	−0.159 ± 0.010	0.054 ± 0.004
Cu	−0.093 ± 0.006	−0.094 ± 0.025	0.045 ± 0.007
Zn	−0.048 ± 0.006	−0.038 ± 0.025	0.039 ± 0.006

Notes. [a][X/H] derived with HET data, relative to the Sun.
[b][X/H] derived with CFHT data, relative to the Sun.
[c]Δ[X/H] derived with respect to Kepler-10 (HET).

coefficient is $r_S = +0.68$ when using T_c, but only −0.32 for the FIP. The probability of a correlation arising by chance is 0.2 per cent for T_c, while the probability of the correlation with FIP arise by chance is 20.6 per cent. We emphasize that there is no convincing physical scenario to explain the FIP trend in our results. The FIP effect modifies only the chromospheric and coronal abundances in the Sun, not the photospheric abundances, which is of relevance here.

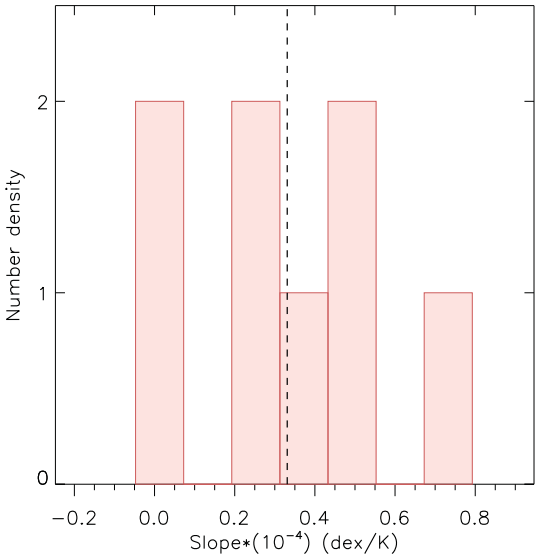

Figure 8. Histogram of the slopes when applying a single linear fit to Δ[X/H]–T_c correlations for the eight thick disc stellar twins. The black dashed vertical line represents the location of the mean value of Δ[X/H] versus T_c slopes.

Already in discussing Fig. 4 above, we could draw the conclusion that clear correlations with condensation temperature exist for the abundances of Kepler-10 relative to its twins. We have studied this further by applying the linear fits of [X/H] versus [Fe/H], but using 'Twins - Kepler-10' for self-consistency, to correct the abundances of each twin to the [Fe/H] of Kepler-10 and thus derived GCE-corrected results. The corrections are relatively small, reflecting the small range in [Fe/H] of the twins. When plotting the differences between these corrected abundances and those of Kepler-10 versus T_c we obtain a diagram (see Fig. 11) similar to Fig. 6, though with a

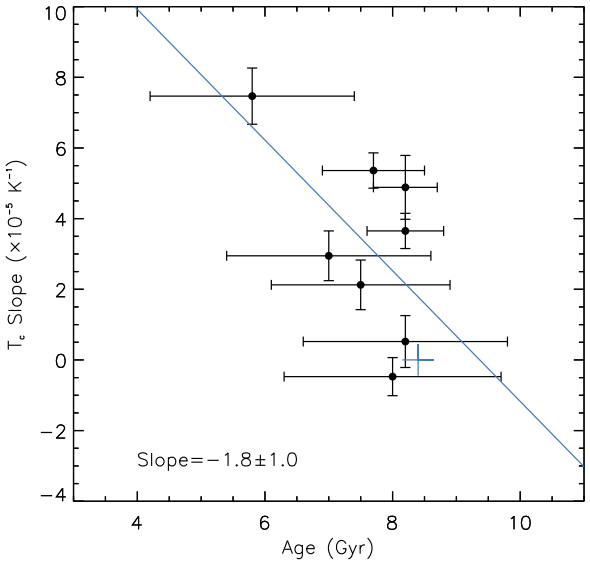

Figure 9. Gradient for a single linear fit to Δ[X/H] versus T_c slopes as a function of stellar ages for thick disc stars. Δ[X/H] were measured using Kepler-10 as a reference. The blue solid line represents the linear fit for the thick disc stars. The location of Kepler-10 is marked with blue cross.

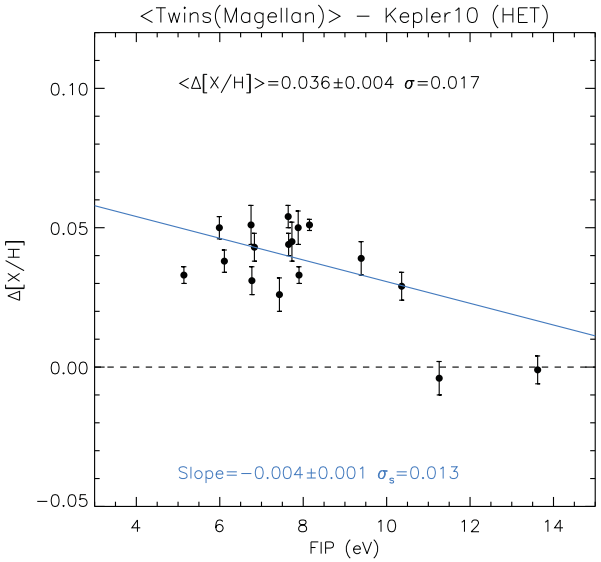

Figure 10. Differential chemical abundances Δ[X/H] as a function of FIP. The blue solid line represents the linear fit to the data, σ_s is the dispersion about the linear fit.

slightly flatter gradient [$(0.24 \pm 0.03) \times 10^{-4}$ K^{-1}] and a marginally larger scatter. Obviously, these GCE corrections cannot erase the Δ[X/H]–T_c trend.[4] One concern regarding the GCE corrections in our analysis is that we are correcting the GCE effects using the abundance ratios–[Fe/H] relations, as was done by Adibekyan et al. (2014). Nissen (2015) demonstrated that age may be a better tracer for the GCE and should be considered when applying the GCE corrections. Indeed a recipe including both age and [Fe/H] could be the best way to estimate the GCE effects. However, the age range

[4] A similar approach using Si as the reference element does not change our results. We find a slope of $(0.214 \pm 0.036) \times 10^{-4}$ K^{-1}, i.e. a 5.9σ result.

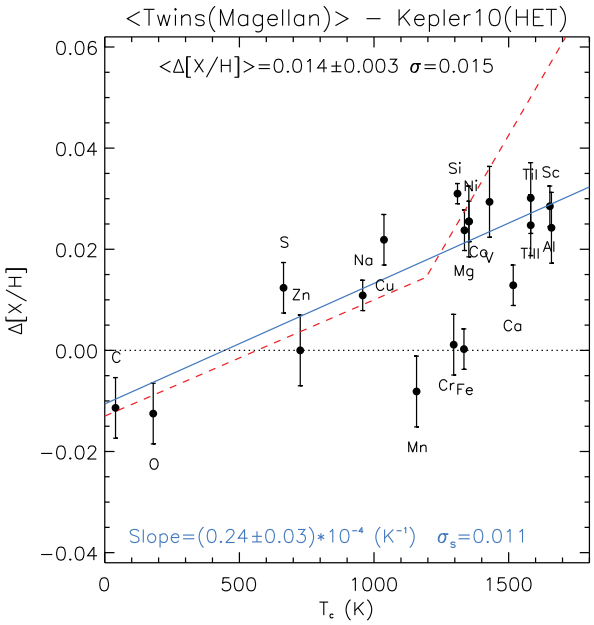

Figure 11. Average abundance differences Δ[X/H] versus condensation temperature T_c for the eight thick disc stellar twins relative to Kepler-10 with GCE corrections applied. The *Y*-axis is the same as in Fig. 6. The blue solid line represents the linear fit to the data, σ_s is the dispersion about the linear fit and the red dashed line is the fit from Meléndez et al. (2009) for solar twins − Sun, normalized to Δ[C/H].

of the Kepler-10 thick disc twins is so narrow that we cannot, and probably do not need to address an accurate GCE correction using the abundance ratio versus stellar age plots. Additional thick disc stellar twins would clarify this situation further.

When comparing Kepler-10 to its eight thick disc stellar twins, we find that Kepler-10 is depleted in refractory elements. The Δ[X/H]–T_c trends vary star to star which complicates the possible scenario. Chemical signatures of terrestrial planet formation, stellar ages, stellar birth locations, GCE effects, variation in dust-depletion in star-forming regions, etc. may affect our results. We notice that each of the scenarios discussed above may not be fully responsible for the observed abundance while a combination of several factors might affect and produce the current chemical composition of Kepler-10 and its stellar twins.

6 CONCLUSIONS

We conducted a line-by-line differential abundance study of Kepler-10 and a sample of stellar twins, obtaining extremely high precision based on spectra from three telescopes (CFHT, HET and Magellan). Our analysis reveals subtle chemical differences in the photosphere of Kepler-10 when compared to its stellar twins. We confirm that Kepler-10 is very likely a thick disc star considering its old age (8.4 ± 1.0 Gyr), kinematic probabilities (96 per cent as thick disc member) and abundance ratios (according to Fig. 4). When comparing Kepler-10 to its thick disc twins, a single linear fit provides an appropriate representation of the Δ[X/H]–T_c trend. We find that Kepler-10 is depleted in refractory elements relative to volatile elements when compared to the majority of thick disc stellar twins. Two of the eight thick disc twins do not show depletion patterns, which is within the small number statistics compatible with Meléndez et al. (2009) and Ramírez et al. (2009, 2010) resulting 15 per cent of solar twins have chemical compositions that match the solar value. The

average abundance difference between thick disc twins and Kepler-10 is 0.037 ± 0.004 (σ = 0.016) which corresponds to at least 13 Earth masses material. One possible explanation could be the formation of terrestrial planets in the Kepler-10 system. However, the results are not as clear as for the solar twins (Meléndez et al. 2009; Ramírez et al. 2010). Other factors (e.g. stellar age, stellar birth location and GCE) might also affect the abundance results.

Naturally the thick disc twins may also harbour similarly large rocky planets as Kepler-10, although they have not yet been detected. Several studies based on current discoveries of exoplanets (Howard, Marcy & Bryson 2012; Petigura, Marcy & Howard 2013; Burke et al. 2015) reported estimations of occurrence rate of rocky planets around different type of stars with different orbits. Petigura et al. (2013) indicate that at least one in six stars might host a planet with 1–2 R_E with period between 5–50 d. In this case, the peculiar chemical composition of Kepler-10 could reveal signatures regarding the different planetary masses, orbits, formation efficiency or formation time-scale. In order to test the Meléndez et al. (2009) scenario regarding terrestrial planet formation and unravel the possible subtle chemical signatures and better understand the mechanisms of planet formation, more spectra of terrestrial planets host stars and their identical stellar twins with high SNR (>350) are needed. It is also important to conduct similar analysis with binary stars (e.g. Liu et al. 2014; Mack et al. 2014; Tucci Maia et al. 2014; Biazzo et al. 2015; Ramírez et al. 2015; Saffe et al. 2015; Teske et al. 2015) or open cluster stars (e.g. Brucalassi et al. 2014; Önehag et al. 2011, 2014; Spina et al. 2015) since these systems presumably share the identical initial chemical composition, thus making them ideal targets for tracing small differential abundance differences that could reveal different formation histories of the individual stars and their planets.

ACKNOWLEDGEMENTS

This work has been supported by the Australian Research Council (grants FL110100012, FT140100554 and DP120100991). JM thanks support by FAPESP (2012/24392-2). DLL thanks the Robert A. Welch Foundation of Houston, Texas for support through grant F-634. TB was supported by the project grant 'The New Milky Way' from the Knut and Alice Wallenberg Foundation. Australian access to the Magellan Telescopes was supported through the Collaborative Research Infrastructure Strategy of the Australian Federal Government. The Canada–France–Hawaii Telescope is operated by the National Research Council of Canada, the Institut National des Sciences de l'Univers of the Centre National de la Recherche Scientifique of France, and the University of Hawaii. The Hobby–Eberly Telescope is a joint project of the University of Texas at Austin, the Pennsylvania State University, Ludwig-Maximilians-Universität München, and Georg-August-Universität Göttingen.

REFERENCES

Adibekyan V. Z., González Hernández J. I., Delgado Mena E., Sousa S. G., Santos N. C., Israelian G., Figueira P., Bertran de Lis S., 2014, A&A, 564, L15
Asplund M., 2005, ARA&A, 43, 481
Asplund M., Grevesse N., Sauval A. J., Scott P., 2009, ARA&A, 47, 481
Batalha N. M. et al., 2011, ApJ, 729, 27
Bedell M., Meléndez J., Bean J. L., Ramrez I., Leite P., Asplund M., 2014, ApJ, 795, 23
Bensby T., Feltzing S., Lundström I., Ilyin I., 2005, A&A, 433, 185
Bensby T., Feltzing S., Oey M. S., 2014, A&A, 562, 71
Bernstein R., Shectman S. A., Gunnels S. M., Mochnacki S., Athey A. E., 2003, in Iye M., Moorwood A. F. M., eds, Proc. SPIE Conf. Ser. Vol. 4841, Instrument Design and Performance for Optical/Infrared Ground-based Telescopes. SPIE, Bellingham, p. 1694
Biazzo K. et al., 2015, A&A, 583, 135
Brucalassi A. et al., 2014, A&A, 561, 9
Burke C. J. et al., 2015, ApJ, 809, 8
Castelli F., Kurucz R. L., 2003, in Piskunov N., Weiss W. W., Gray D. F., eds, Proc. IAU Symp. 210, Astron. Soc. Pac., San Francisco, p. A20
Chambers J. E., 2010, ApJ, 724, 92
Dumusque X. et al., 2014, ApJ, 789, 154
Epstein C. R., Johnson J. A., Dong S., Udalski A., Gould A., Becker G., 2010, ApJ, 709, 447
Feldman U., Laming J. M., 2000, Phys. Scr., 61, 222
Gaidos E., 2015, ApJ, 804, 40
González Hernández J. I., Israelian G., Santos N. C., Sousa S., Delgado-Mena E., Neves V., Udry S., 2010, ApJ, 720, 1592
Howard A. W., Marcy G. W., Bryson S. T., 2012, ApJS, 201, 15
Johnson D. R. H., Soderblom D. R., 1987, AJ, 93, 864
Kim Y. C., Demarque P., Yi S. K., Alexander D. R., 2002, ApJS, 143, 499
Kurucz R., Bell B., 1995, Kurucz CD-ROM No 23. Smithsonian Astrophysical Observatory, Cambridge
Liu F., Asplund M., Ramírez I., Yong D., Meléndez J., 2014, MNRAS, 442, L51
Lodders K., 2003, ApJ, 591, 1220
Mack C. E., III, Schuler S. C., Stassun K. G., Norris J., 2014, ApJ, 787, 98
Manset N., Donati J. F., 2003, in Silvano F., ed., Proc. SPIE Conf. Ser. Vol. 4843, Polarimetry in Astronomy. SPIE, Bellingham, p. 425
Meléndez J., Asplund M., Gustafsson B., Yong D., 2009, ApJ, 704, L66
Meléndez J. et al., 2012, A&A, 543, A29
Neves V., Santos N. C., Sousa S. G., Correia A. C. M., Israelian G., 2009, A&A, 497, 563
Nissen P. E., 2015, A&A, 579, A52
Önehag A., Korn A., Gustafsson B., Stempels E., VandenBerg D. A., 2011, A&A, 528, A85
Önehag A., Gustafsson B., Korn A., 2014, A&A, 562, A102
Petigura E. A., Marcy G. W., Howard A. W., 2013, ApJ, 770, 69
Ramírez I., Meléndez J., 2005, ApJ, 626, 446
Ramírez I., Allende Prieto C., Lambert D. L., 2007, A&A, 465, 271
Ramírez I., Meléndez J., Asplund M., 2009, A&A, 508, 17
Ramírez I., Asplund M., Baumann P., Meléndez J., Bensby T., 2010, A&A, 521, 33
Ramírez I., Meléndez J., Cornejo D., Roederer I. U., Fish J. R., 2011, ApJ, 740, 76
Ramírez I., Allende Prieto C., Lambert D. L., 2013, ApJ, 764, 78
Ramírez I. et al., 2014, A&A, 572, A48
Ramírez I. et al., 2015, ApJ, 808, 13
Reddy B. E., Lambert D. L., Allende Prieto C., 2006, MNRAS, 367, 1329
Rogers L. A., 2015, ApJ, 801, 41
Saffe C., Flores M., Buccino A., 2015, A&A, 582, A17
Santos N. C. et al., 2015, A&A, 580, L13
Siess L., Dufour E., Forestini M., 2000, A&A, 358, 593
Sneden C., 1973, ApJ, 184, 839
Sobeck J. S. et al., 2011, AJ, 141, 175
Sousa S. G., Santos N. C., Israelian G., Mayor M., Monteiro M. J. P. F. G., 2007, A&A, 469, 783
Spina L. et al., 2015, A&A, 582, L6
Teske J. K., Ghezzi L., Cunha K., Smith V. V., Schuler S. C., Bergemann M., 2015, ApJ, 801, 10
Tucci Maia M., Meléndez J., Ramírez I., 2014, ApJ, 790, L25
Tull R. G., 1998, in Sandro D., ed., Proc. SPIE Conf. Ser. Vol. 3355, Optical Astronomical Instrumentation. SPIE, Bellingham, p. 387
Yi S. K., Demarque P., Kim Y. C., Lee Y.-W., Ree C. H., Lejeune T., Barnes S., 2001, ApJS, 136, 417
Yong D. et al., 2013, MNRAS, 434, 3542

SUPPORTING INFORMATION

Additional Supporting Information may be found in the online version of this article:

Table A1. Atomic line data used for our abundance analysis.
Table A2. Δ[X/H] for each programme star with relative to Kepler-10 (http://www.mnras.oxfordjournals.org/lookup/suppl/doi:10.1093/mnras/stv2821/-/DC1).

Please note: Oxford University Press is not responsible for the content or functionality of any supporting materials supplied by the authors. Any queries (other than missing material) should be directed to the corresponding author for the article.

This paper has been typeset from a TEX/LATEX file prepared by the author.